Analyst

PAPER

View Article Online
View Journal

Cite this: DOI: 10.1039/c7an01295k

A ratiometric electrochemical strategy for sensitive determination of Furin activity based on dual signal amplification and antifouling nanosurfaces†

Dazhi Yao, Wenqi Zhao, Limin Zhang * and Yang Tian *

Developing a sensitive and accurate method for Furin activity is still the bottleneck for understanding the role played by Furin in cell-surface systems and even in Alzheimer's disease. In this work, a ratiometric electrochemical biosensor was developed for sensitive and accurate determination of Furin activity in the cell based on dual signal amplification stemming from a peptide with multiple response sites and the antifouling gold nano-bellflowers (GBFs). A new peptide, HS-CMRVRR↓YKDFDFG (P3), was designed for the first time to be selectively cleaved by Furin at site↓. More importantly, this peptide P3 constitutes three amino acid residues with the –COOH group subsequently used to bind with the response molecule of ferrocene, and can remarkably improve the determination sensitivity by about 2.3 fold. Meanwhile, GBFs stabilized by PEG were taken as a second element to magnify the signal of the ferrocene group *via* a large ratio surface area and good conductivity, as well as an antibiofouling nanosurface to reduce the biofouling of the electrode surface in cells. This double amplification strategy can greatly enhance the sensitivity of Furin detection by 6.5-fold, which is favorable for detection of low amounts of Furin. In addition, 5′-MB-GGCGCGA$(T)_{13}$-SH-3′ was co-assembled as an inner reference to provide a built-in element to correct the determination error resulting from a complicated analysis environment. Finally, this sensitive and accurate Furin biosensor was successfully applied to detect Furin activity in Furin overexpressed U251 and MDA-MB-468 cells. As far as we know, this is the first report to mention an electrochemical strategy to detect Furin activity in cells.

Received 4th August 2017,
Accepted 26th September 2017

DOI: 10.1039/c7an01295k

rsc.li/analyst

Introduction

As one of the important endoproteases, Furin is a protein in humans encoded by the Furin gene which processes numerous physiological substrates.[1–4] It can activate a variety of protein precursors in intracellular membrane and cell-surface systems, and process them into biologically functional peptides and proteins.[5,6] More importantly, the activation of α- and β-secretases, two key enzymes in processing the generation of toxic amyloidal peptides during the development of Alzheimer's disease, was also found to be mediated by the proteolytic activities of Furin.[7–9] Therefore, developing a sensitive, and accurate approach to detect Furin in cells is very important for understanding the function of Furin in cells and related diseases.

Until now, some elegant approaches have been established for determination of Furin, including fluorescence sensors, nuclear magnetic resonance imaging, and photoacoustic imaging.[10–14] Though electrochemical methods have been widely developed for detection of enzymes and proteins due to their remarkable advantages of sensitivity, being simple and a low-cost measurement system,[15–19] as far as we know, there is hitherto no electrochemical probe reported for the detection of Furin. Two main large challenges are considered to block the electrochemical analysis of Furin. On the one hand, Furin lacks electroactive centres, and hence it is difficult to directly determine Furin relying on its inherent electrochemical response. On the other hand, an enduring hindrance in the elaboration of electrochemical devices for enzyme determination like Furin in practical biological samples is the surface biofouling originating from the nonspecific adsorption of the enzyme itself and biological substances on the electrode surface, and distinct determination environments between *in vitro* experiments and in practical samples.[20–23] The nonspecific surface adsorption can inactivate the electrode, making electrochemical sensors suffer from a larger determination error due to invalidation of the as formed method operated in *in vitro* experiments.

Recently, ratiometric strategies have been demonstrated to be an efficient way to enhance the accuracy of determination.[24–27] Compared to traditional electrochemical

Department of Chemistry, School of Chemistry and Molecular Engineering, East China Normal University, Dong Chuan Road 500, Shanghai 200241, P.R. China. E-mail: lmzhang@chem.ecnu.edu.cn, ytian@chem.ecnu.edu.cn

†Electronic supplementary information (ESI) available. See DOI: 10.1039/c7an01295k

sensors with a single-electric signal output, ratiometric sensors with dual-electric signal outputs can efficiently correct the inaccuracy from complicated biological environments because the ratiometric intensities from dual signals are independent of the sensor or reagent concentrations.[28–30] However, this ratiometric determination model cannot eliminate biofouling. Particularly for enzyme determination, some incubation time is necessary, during which biological molecules have readily spontaneously adsorbed on the electrode surface, resulting in the loss of the electric signal. In addition, a large response signal of the ratiometric electrochemical sensor was also pursued to simultaneously enhance the sensitivity and accuracy of the electrode, which is pivotal to detect target molecules in low concentration or amount, like Furin. This is pivotal to detect low amount target molecules, like Furin.[8] For this purpose, various nanomaterials were generally modified on the electrode to amplify the response signal through increasing the ratio surface area. However, this amplification efficiency simply relying on nanomaterials is still limited.

In this work, we developed an integrated organic–inorganic interface for detection of Furin, using gold nano-bellflowers (GBFs) with PEG as the antifouling element, a peptide with multiple response sites as specific recognition as shown in Scheme 1. Three new strategies were designed: (i) a new peptide recognition was designed to selectively detect Furin with the following composition: HS-CMRVRR↓YKDFDFG (denoted as P3), in which the site indicated by ↓ can be selectively cleaved by Furin, and the thiol side of P3 is used to assemble P3 at the Au nanostructure. The other side of P3 constitutes three amino acid residues with the –COOH group, D, D, and G, which are subsequently used to bind with the electroactive molecule, aminoferrocene (NH_2-Fc). After Furin selectively cut at the –RR site, the peak current of ferrocene decreases. Compared with the peptide with only one site to bind NH_2-Fc (denoted as P1), P3 can remarkably improve the determination sensitivity for about 2.3 fold; (ii) GBFs stabilized by PEG molecule as the antifouling element were synthesized to play two roles: one, a conductive and antifouling nanosurface for detection of furin; two, a second element to amplify the signal of the ferrocene group *via* a large ratio surface area originating from the nanostructure with abundant branches. Employing these GBFs, the sensitivity of Furin detection was enhanced by approximately 3.8-fold. (iii) Meanwhile, 5′-MB-GGCGCGA$(T)_{13}$-SH-3′ (MB-DNA-SH, MB = Methylene Blue) was co-assembled as an inner reference to provide a built-in element to correct the determination error resulting from complicated determination environments. To the best of our knowledge, this is the first electrochemical probe for Furin determination.

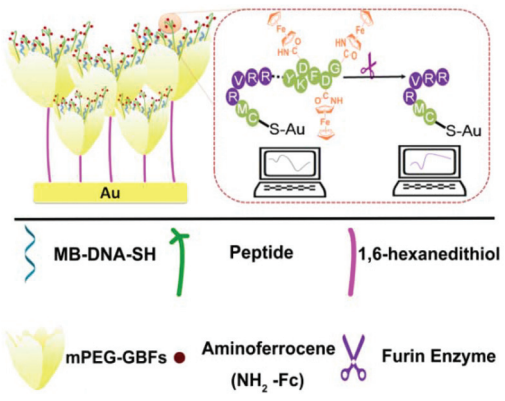

Scheme 1 Illustration of the electrochemical biosensor for detection of the activity of Furin based on dual amplifications.

Experimental

Materials and chemicals

NH_2-Fc was purchased from Tokyo Chemical Industry Co., Ltd. Gold(III) chloride trihydrate ($HAuCl_4 \cdot 3H_2O$, 99%), 1,6-Hexanedithiol, *o*-phenetidine,1-ethyl-3-(3 dimethyl-aminopropyl)carbodiimide (EDC), *N*-hydroxysuccinimide (NHS), glucose oxidase, glucose, ATP, tyramine, all amino acids, trypsin, carboxylesterase, cytochrome C, and Furin Inhibitor were purchased from Sigma Aldrich (U.S.A). KCl, NaCl, $CaCl_2$, $MgCl_2$, $FeCl_3$, $ZnCl_2$, $CuCl_2$, Na_2HPO_4 and NaH_2PO_4 were obtained from sinopharm chemical reagent Co. Ltd. The definition of Furin activity is that one unit will release 1 pmol of AMC from the fluorogenic peptide Boc-RVRR-MCA per minute at 30 °C. MB-DNA-SH was bought from Shanghai Shenggong. Peptide "Cys-Met-Arg-Val-Arg-Arg-Tyr-Lys-Phe-Gly" (CMRVRRYKFG, abbreviated as P1) and peptide "HS-Cys-Met-Arg-Val-Arg-Arg-Tyr-Lys-Asp-Phe-Asp-Gly" (CMRVRR↓YKDFDG, abbreviated as P3) were obtained from Shanghai Biotech Bioscience and Technology Co., Ltd, China. Except for acetonitrile (SP) used in HPLC, all the reagents and materials were commercially available and at least of analytical grade. Aqueous solutions were prepared with ultrapure water (18.2 MΩ cm^{-1}) from a Millipore water purification system.

Synthesis of gold bellflowers (GBFs)

Gold bellflowers (GBFs) were synthesized as reported previously.[31,32] Firstly, 5 mL of 0.8 mol L^{-1} $HAuCl_4$ aqueous solution was heated at 50 °C for 5 min, and then 10 μL *o*-phenetidine dissolved in 4 mL hexane was gently added on top of the $HAuCl_4$ aqueous solution. Afterward, the two-phase system was sonicated at 50 °C for 30 min and then the system was transferred to an ice bath with the same sonication condition for another 60 min. The product was collected by centrifugation at 9000 rpm for 10 min and was washed three times with deionized water. After that, 100 μL of 10 mmol L^{-1} HS-PEG-NH_2 (MW = 3400) solution was added. The reaction mixture was stirred at room temperature for another 2 h. The mixture was centrifuged and washed three times with deionized water to obtain PEGylated GBFs in aqueous solution.

Preparation and modification of the electrode

The gold electrode surface was first mechanically polished with alumina powders of 0.1 μm, and 0.05 μm, respectively, until a mirror-like surface was obtained. The electrode was

rinsed and sonicated with deionized water, acetone and deionized water sequentially to remove any impurities including adhering alumina. The gold electrode, then, was electrochemically cleaned in 0.5 mol L^{-1} H_2SO_4 solution in the potential range of −0.2 and 1.5 V *vs.* Ag/AgCl. After that, the electrode was rinsed with deionized water. First of all, the GBFs were linked on the pretreated gold electrode with 1,6-hexanedithiol, which was denoted as Au/GBF. Then, the Au/GBF electrode was soaked in 10 mM PBS solution containing 10 mM MB-DNA-SH and 5 mM P3 at a temperature of 4 °C for 12 h, and the modified electrode was denoted as Au/GBF/MB + P3. Finally, the NH_2-Fc was coordinated on the Au/GBF/MB + P3 electrode in ethanol solution of NH_2-Fc (1 mg mL^{-1}) using EDC and NHS as catalysts. The resulting electrode is denoted as GBF/MB + P3/Fc electrode.

Cell culture and cell lysate assay

Human Neuronal Glioblastoma U251 Cells and human breast cancer MDA-MB-468 cells were maintained in Dulbecco's modified Eagle's medium supplemented with 10% fetal bovine serum and grown at 37 °C in a humidified incubator (5% CO_2–95% air). Human colorectal adenocarcinoma Lovo cells were grown in F-12 K medium with 10% FBS. Cells were carefully trypsinized and centrifuged (800 rpm for 3 min) to remove medium, and washed with PBS buffer. Then RIPA buffer (Sigma, containing 150 mM NaCl, 1.0% IGEPAL® CA-630, 0.5% sodium deoxycholate, 0.1% SDS, and 50 mM Tris, and pH 8.0) was added and kept on ice for 1 h. The lysates were collected and centrifuged at 14 000 rpm for 5 min to remove insoluble substances. Then, 100 μL cell lysate were diluted to 10 mL solution with 10 mM PBS buffer (pH 7.4). Finally, various modified electrodes were dipped in the diluted lysate and incubated at 37 °C for 15 minutes before determination.

Instruments and measurements

The electrodes for electrochemical experiments were purchased from Shanghai Chenhua Co., Ltd, China. Electrochemical experiments were performed on an computer-controlled CHI660a (Shanghai, China) electrochemistry workstation in deaerated aqueous 10 mM PBS solution with a three-electrode configuration, in which all modified gold electrodes were used as the working electrode, a Pt wire as the counter electrode and a Ag/AgCl electrode as the reference electrode. All measurements were carried out at ambient temperature. Differential pulse voltammetry (DPV) parameters were selected as follows: potential step of 4 mV, pulse width of 0.05 s, pulse period of 0.5 s, and pulse amplitude of 50 mV. The ultraviolet-visible absorbance spectrum was obtained using a Hitachi-5300. X-ray Photoelectron spectroscopy (XPS) investigations were conducted in an AXIS Ultra DLD system (Shimaduza, Japan) to figure out the process of modification. HR-TEM images were taken on a JEM-2100F and the X-ray diffraction (XRD) pattern was obtained on a Shimadzu XRD-6000. Analytical reverse-phase HPLC analysis was performed on a Shimadzu HPLC system with an Alltima-C18 column at a flow rate of 0.20 mL min^{-1}.

Results and discussion

Characterization of the GBFs and modified electrodes

At first, GBFs were synthesized through a liquid–liquid–gas triphase interface system produced by ultrasound induced vacuum bubbles in a two-phase liquid–liquid system as previously reported.[31,32] The defined bellflower shape with multiple-branched petals over about 20 and narrow gaps (1–4 nm) between adjacent petals is shown in Fig. 1A. Furthermore, GBFs were well dispersed and have a uniform size, 100 ± 50 nm (Fig. 1B). The corresponding optical properties of the aqueous dispersions were characterized by UV-vis spectroscopy (Fig. S1, ESI†). The particles exhibited a strong plasmon peak around 850 nm, which is consistent with previous reports.[31,32] The observed lattice fringe of 0.2355 nm in the high-resolution TEM image (Fig. 1C) corresponds to the (111) lattice planes in GBFs and the lattice fringe of 0.2039 nm is identical to the (200) lattice plane. The crystalline orientation of GBFs was further characterized by X-ray Power Diffraction (XRD) (Fig. 1D). Five featured peaks, located at 39.0°, 45.2°, 65.5°, 78.6 and 82.1, were observed, which correspond to (111), (200), (220), (311) and (222) facets, respectively.

Each step of electrode modification was also tracked by X-ray spectroscopy (XPS) (Fig. S2, ESI†). At the 1, 6-hexanedithiol (HDT) modified Au electrode, two peaks at 83.2 eV and 86.8 eV represent Au $4f_{7/2}$ and Au $4f_{5/2}$, respectively (Curve a of Fig. S2A, ESI†). Meanwhile, two S 2p peaks demonstrated successful modification of HDT, in which the S $2p_{2/3}$ peak located at 163.2 eV was ascribed to unbound alkanethiol and that observed at 165 eV was attributed to the self-assembled thiol group from HDT onto the gold surface (Curve b of Fig. S2B, ESI†). The S peak located at 163.2 eV disappeared after GBFs were immobilized at the Au electrode surface due to formation of the S–Au bond between GBFs and unbound thiol groups

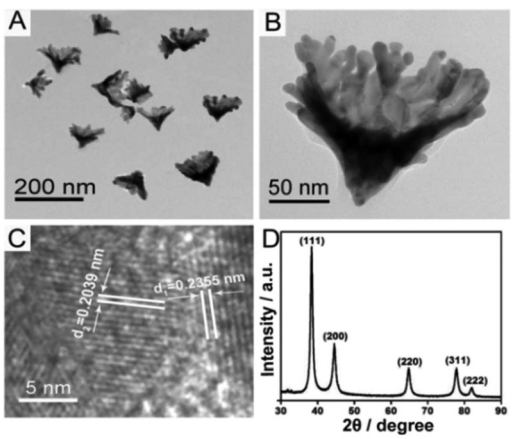

Fig. 1 (A) Representative TEM image of GBFs, (B) their enlarged TEM image, (C) enlarged HRTEM image of GBFs and (D) XRD pattern of GBFs.

(Curve c of Fig. S2B, ESI†). When MB-DNA-SH and P3 were co-assembled on the Au/GBF electrode (denoted as Au/GBF/MB + P3), the P 2p peak located at 133.7 eV indicated the modification of MB on GBFs (Curve c of Fig. S2C, ESI†). Finally, NH_2-Fc was assembled at the Au/GBF/MB + P3 electrode. The resulting electrode was denoted as GBF/MB + P3/Fc. The Fe $2p_{3/2}$ peak at 708.2 eV and the Fe $2p_{1/2}$ peak at 720.3 eV were clearly observed as expected. These observations demonstrate that P3 and NH_2-Fc have been immobilized on the electrode (Curve d of Fig. S2D, ESI†).

Electrochemical response of the GBF/MB + P3/Fc electrode

Differential pulse voltammetry (DPV) was employed for quantitative determination of Furin activity in 10 mM PBS (pH 7.4). As demonstrated in Fig. 2A, only one cathodic peak at −212 mV *versus* Ag/AgCl was clearly observed at the Au/GBF/MB + P3 electrode (Curve c in Fig. 2A), while no peak was obtained at bare Au and Au/GBF (Curves a and b in Fig. 2A). These results demonstrated that the peak at −212 mV was attributed to the reduction of the MB group in MB-DNA-SH. After NH_2-Fc molecules were further coordinated with the –COOH groups of P3 at the Au/GBF/MB + P3 electrode, a new cathodic peak was observed at *ca.* 195 mV *versus* Ag/AgCl (Curve d, Fig. 2A) in PBS solution (pH 7.4), as a consequence of reduction of the ferrocene group. This peak potential of the ferrocene group is well separated from that of MB. After being kept in PBS (pH 7.4) for 120 min, a small deviation of J_p/J_p^0 (the peak current density ratio obtained at 195 mV and −212 mV), <5%, means good stability of the GBF/MB + P3/Fc electrode (Fig. S3, ESI†). After Furin was added into the PBS solution, the peak current of ferrocene at 195 mV decreased due to the selective cleavage of P3 by Furin at the –RR site.

This enzyme cleavage effect was further confirmed *via* HPLC analysis (Fig. S4, ESI†). One peak is observed when only P3 existed (Curve a in Fig. S4, ESI†), while two peaks appeared in the mixture of P3 after incubation with Furin for 30 minutes (Curve b in Fig. S4, ESI†), which were attributed to two pieces of P3 cleaved by Furin. As a control, the mixture of P3, Furin, and Furin inhibitor was also tested. As anticipated, only one peak was obtained when the Furin inhibitor was added. These results indicate that P3 was successfully cleaved by Furin. According to the plot of cathodic peak current with time, the reaction time for the cleavage of Furin was optimized at 15 min (Fig. S5, ESI†). Then, the electrochemical behavior was recorded at the GBF/MB + P3/Fc electrode with different concentration ratios of MB-DNA-SH and P3 ($C_{MB}:C_{P3}$) (Fig. S6, ESI†), and the $C_{MB}:C_{P3}$ of 2 : 1 was finally selected. In addition, the cathodic peak current intensity (J_p) at ~195 mV gradually decreased with increasing activity of Furin. Besides, moreover, the J_p/J_p^0 values exhibited a good linearity with the concentration of Furin in the range of 1 to 50 U L^{-1} with a detection limit down to 0.8 U L^{-1} (S/N = 3 : 1) (inset of Fig. 2B).

Comparison in performance between dual amplification and non-amplification sensors

To evaluate the amplification effect of GBFs, the MB and P3 modified Au electrode (Au/MB + P3/Fc) was prepared as a control electrode to detect Furin. The amplification factor was estimated according to the peak current ratio of ferrocene at GBF/MB + P3/Fc to that of at Au/MB + P3/Fc. As shown in Fig. 3a, the peak current of ferrocene obtained at GBF/MB + P3/Fc was estimated to be *ca.* 3.8-fold larger than that obtained at Au/MB + P3/Fc owing to the amplified effect of GBFs. In addition, the peptide with a single amino acid site with –COOH, P1, was used as a control to evaluate the amplification effect of P3. As shown in Fig. 3b, the J_p/J_p^0 value at the GBF/MB + P3/Fc electrode is nearly 2.3 times that obtained at GBF/MB + P1/Fc, suggesting that the designed P3 peptide can effectively improve the peak current of ferrocene. It is worth mentioning that the amplification factor of 2.3 times is slightly smaller than expected 3.0 times. Such distinction might result from the incomplete coordination of P3 with NH_2-Fc.

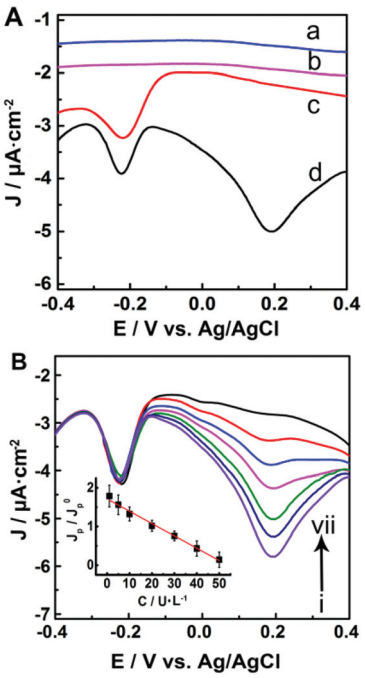

Fig. 2 (A) DPVs obtained at (a) bare Au, (b) Au/GBF, (c) Au/GBF/MB + P3, (d) GBF/MB + P3/Fc in 10 mM PBS (pH 7.4) and (B) DPVs of the GBF/MB + P3/Fc electrode in 10 mM PBS with different activities of Furin. They are 1, 5, 10, 20, 30, 40, and 50 U L^{-1} from i to vii, respectively. Inset: The linear plot of J_p/J_p^0 with Furin activity.

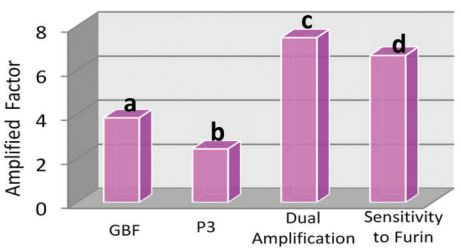

Fig. 3 Amplification factor by (a) GBFs, (b) P3, (c) dual amplification, and (d) sensitivity to Furin.

Compared with the single amplification situation, a larger amplification factor, ~7.1, was obtained when GBF and P3 were simultaneously employed for double amplification of the ferrocene electric signal (Fig. 3c). This double amplification strategy apparently enhanced the sensitivity for Furin detection by ~ 6.5 fold, compared to that of the MB and P1 co-assembled Au electrode (Au/MB + P1/Fc) (Fig. 3d, and Fig. S7, ESI†).

Next, the antifouling capability of PEGlysated GBFs was evaluated through comparison of the DPV responses obtained at Au/MB + P3/Fc and GBF/MB + P3/Fc electrodes. The $J_p^{0\prime}/J_p^0$ value ($J_p^{0\prime}$ stand for the current density of MB dipped in cell lysate for different time, J_p^0 is the initial current density of MB) obtained at Au/MB + P3/Fc greatly decreased by ~49% after successive determination for 2 h in Lovo cell lysate. In contrast, only 16% decrease of $J_p^{0\prime}/J_p^0$ value was attained at GBF/MB + P3/Fc electrode (Fig. S8, ESI†). These results demonstrated that the PEGlysated gold bellflower can effectively defend the biofouling from practical cell environments.

More importantly, in order to confirm the accuracy of ratiometric GBF/MB + P3/Fc in a practical cell environment, we further compared the alternation of the electrochemical signal under the situation with and without the MB inner reference. Lovo cell lysate with a negligible Furin amount was taken as the evaluation environment. As shown in Fig. 4, the peak current densities of MB and ferrocence were both decreased by ~16% within successive determination within 4 h in Lovo cell lysate due to biofouling. In contrast, J_p/J_p^0 almost remains constant. These results clearly demonstrate that the ratiometric GBF/MB + P3/Fc electrode can greatly improve the accuracy for Furin detection in cell lysate.

Determination of Furin activity in cells

The complexity of the cell system also represents a significant challenge for analytical performance not only in terms of sensitivity and accuracy, but importantly in terms of selectivity. The selectivity of designed peptide for Furin over other potential coexisting species, including metal ions, amino acids, biological molecules, and typical enzymes including glucose oxidase, trypsin, catalase, carboxylesterase, and tyrosinase, was evaluated (Fig. S9, ESI†). No obvious change in $\Delta(J_p/J_p^0)$ (<5%) was observed upon the addition of various metal ions, amino acids, and proteins. Such remarkable selectivity displayed by the Furin biosensor is attributed to the specific cleavage of the -RVRR- peptide only by Furin.

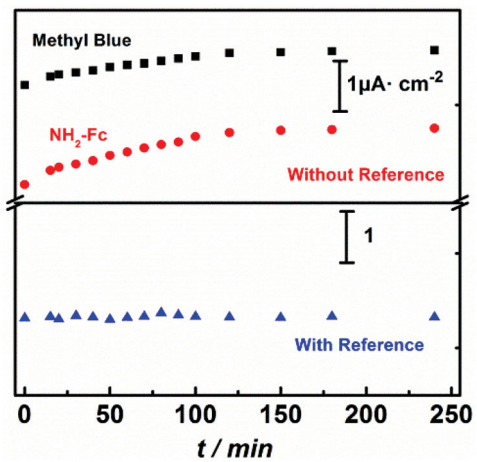

Fig. 4 Comparative performance of electrodes with the inner reference and without the inner reference: the upper one is the current of NH_2-Fc and MB at the GBF/MB + P3/Fc electrode in Lovo cell lysate with time; below is the peak current density ratio J_p/J_p^0 with time obtained at the GBF/MB + P3/Fc electrode in Lovo cell lysate with time.

Table 1 The activity of Furin in different cell lysates

Cell	Number of cells	Total activity of Furin (U L^{-1})	Average activity of Furin in single cell (mU L^{-1})
U251	10^3	2.53 ± 0.59	2.65 ± 0.61
	10^4	27.78 ± 6.38	
MDA-MB-468	10^3	1.89 ± 0.57	1.79 ± 0.53
	10^4	16.92 ± 4.94	
Lovo cell	10^3	N.A.	N.A.
	10^4	N.A.	

With more accurate and sensitive performance of the electrode, the present ratiometric approach based on dual signal amplification of GBFs and peptide with multiple response sites was applied to detect Furin activity in two kinds of Furin overexpressed cells: U251 and MDA-MB-468. The results are listed in Table 1. The Furin level in these cell lysates is 2.65 ± 0.61 mU L^{-1} in U251 cell lysate, and 1.79 ± 0.53 mU L^{-1} in MDA-MB-468 lysate. As a control, the present approach was also applied to detect Furin in lovo cells. Furin cannot be determined, suggesting that the Furin amount in lovo cell lysate is too low to be detected. The activity of Furin was also measured by the traditional Elisa method, (Table S1, ESI†). The concentrations of the electrochemical sensor coincided well with those monitored by the Elisa method. These results demonstrated that the present sensor provides an efficient way to determine Furin in low amounts in biological systems.

Conclusions

In summary, by combination of new peptide P3 composed of multiple response sites and selective cleavage sites with gold nano-bellflowers, a sensitive electrochemical strategy for detection of Furin activity has been developed. This novel double signal amplification originating from the peptide and nanomaterial can greatly enhance the sensitivity for determination of low amount Furin activity. In addition, the present single biosensor demonstrated good selectivity against potential interference in cells including metal ions, amino acids, and proteins. More importantly, integration of the antifouling nanosurface and the ratiometric strategy is particularly suitable for detection of enzymes with high accuracy in practical biological samples. The present work not only provides a methodology for designing and constructing accurate biosensors for monitoring the activity of other enzymes, and

small molecules, which play important roles in biological system, but also establishes a new platform to sensitively and accurately detect targets in low amounts.

Conflicts of interest

There are no conflicts to declare.

Acknowledgements

The authors greatly appreciate the financial support from the NSFC (21635003 for Y. T.; 21305104, 21545002, and 21675054 for L. Z.), and NSFC for distinguished Young Scholars (21325521 for Y. T.) and this work was partially Supported by Open Funding Project of the State Key Laboratory of Bioreactor Engineering.

Notes and references

1 S. O. Dahms, M. Arciniega, T. Steinmetzer, R. Huber and M. E. Than, *Proc. Natl. Acad. Sci. U. S. A.*, 2016, **113**, 11196–11201.
2 M. Fromer, P. Roussos, S. K. Sieberts, J. S. Johnson, D. H. Kavanagh, T. M. Perumal, D. M. Ruderfer, E. C. Oh, A. Topol, H. R. Shah, L. L. Klei, R. Kramer, D. Pinto, Z. H. Gumus, A. E. Cicek, K. K. Dang, A. Browne, C. Lu, L. Xie, B. Readhead, E. A. Stahl, J. Xiao, M. Parvizi, T. Hamamsy, J. F. Fullard, Y.-C. Wang, M. C. Mahajan, J. M. J. Derry, J. T. Dudley, S. E. Hemby, B. A. Logsdon, K. Talbot, T. Raj, D. A. Bennett, P. L. De Jager, J. Zhu, B. Zhang, P. F. Sullivan, A. Chess, S. M. Purcell, L. A. Shinobu, L. M. Mangravite, H. Toyoshiba, R. E. Gur, C.-G. Hahn, D. A. Lewis, V. Haroutunian, M. A. Peters, B. K. Lipska, J. D. Buxbaum, E. E. Schadt, K. Hirai, K. Roeder, K. J. Brennand, N. Katsanis, E. Domenici, B. Devlin and P. Sklar, *Nat. Neurosci.*, 2016, **19**, 1442–1453.
3 N. G. Seidah and A. Prat, *Nat. Rev. Drug Discovery*, 2012, **11**, 367–383.
4 A. Zhou, G. Webb, X. Zhu and D. F. Steiner, *J. Biol. Chem.*, 1999, **274**, 20745–20748.
5 E. M. Hwang, S.-K. Kim, J.-H. Sohn, J. Y. Lee, Y. Kim, Y. S. Kim and I. Mook-Jung, *Biochem. Biophys. Res. Commun.*, 2006, **349**, 654–659.
6 O. Isacson, H. Seo, L. Lin, D. Albeck and A.-C. Granholm, *Trends Neurosci.*, 2002, **25**, 79–84.
7 J. Walter, C. Kaether, H. Steiner and C. Haass, *Curr. Opin. Neurobiol.*, 2001, **11**, 585–590.
8 H. Y. Wang, D. H. S. Lee, M. R. D'Andrea, P. A. Peterson, R. P. Shank and A. B. Reitz, *J. Biol. Chem.*, 2000, **275**, 5626–5632.
9 A. Weidemann, G. König, D. Bunke, P. Fischer, J. M. Salbaum, C. L. Masters and K. Beyreuther, *Cell*, 1989, **57**, 115–126.
10 C.-Y. Cao, Y.-Y. Shen, J.-D. Wang, L. Li and G.-L. Liang, *Sci. Rep.*, 2013, **3**, 1024.
11 A. Dragulescu-Andrasi, S.-R. Kothapalli, G. A. Tikhomirov, J. Rao and S. S. Gambhir, *J. Am. Chem. Soc.*, 2013, **135**, 11015–11022.
12 Q. Miao, X. Bai, Y. Shen, B. Mei, J. Gao, L. Li and G. Liang, *Chem. Commun.*, 2012, **48**, 9738–9740.
13 J. Mu, F. Liu, M. S. Rajab, M. Shi, S. Li, C. Goh, L. Lu, Q.-H. Xu, B. Liu, L. G. Ng and B. Xing, *Angew. Chem., Int. Ed.*, 2014, **53**, 14357–14362.
14 D. Ye, G. Liang, M. L. Ma and J. Rao, *Angew. Chem., Int. Ed.*, 2011, **50**, 2275–2279.
15 Y. Cao, J. Yu, B. Bo, Y. Shu and G. Li, *Biosens. Bioelectron.*, 2013, **45**, 1–5.
16 T.-E. Lin, A. Bondarenko, A. Lesch, H. Pick, F. Cortés-Salazar and H. H. Girault, *Angew. Chem., Int. Ed.*, 2016, **55**, 3813–3816.
17 N. J. Ronkainen, H. B. Halsall and W. R. Heineman, *Chem. Soc. Rev.*, 2010, **39**, 1747–1763.
18 Y. Yu, H. Li, Y. Yang, Y. Ding, Z. Wang and G. Li, *Anal. Chem.*, 2016, **88**, 12287–12293.
19 J. Zhang, Y. Liu, X. Wang, Y. Chen and G. Li, *Biosens. Bioelectron.*, 2015, **74**, 666–672.
20 I. Banerjee, R. C. Pangule and R. S. Kane, *Adv. Mater.*, 2011, **23**, 690–718.
21 C. M. Cardona, S. Mendoza and A. E. Kaifer, *Chem. Soc. Rev.*, 2000, **29**, 37–42.
22 A. Chen and S. Chatterjee, *Chem. Soc. Rev.*, 2013, **42**, 5425–5438.
23 Y. Zheng, T. Hu, C. Chen, F. Yang and X. Yang, *Chem. Commun.*, 2015, **51**, 5645–5648.
24 X. Chai, X. Zhou, A. Zhu, L. Zhang, Y. Qin, G. Shi and Y. Tian, *Angew. Chem., Int. Ed.*, 2013, **52**, 8129–8133.
25 L. Zhang, Y. Han, F. Zhao, G. Shi and Y. Tian, *Anal. Chem.*, 2015, **87**, 2931–2936.
26 H. Li, N. Y. Arroyo-Currás, D. Kang, F. Ricci and K. W. Plaxco, *J. Am. Chem. Soc.*, 2016, **138**, 15809–15812.
27 Y. Luo, L. Zhang, W. Liu, Y. Yu and Y. Tian, *Angew. Chem., Int. Ed.*, 2015, **54**, 14053–14056.
28 C. Ding and Y. Tian, *Biosens. Bioelectron.*, 2015, **65**, 183–190.
29 F. Zhao, L. Zhang, A. Zhu, G. Shi and Y. Tian, *Chem. Commun.*, 2016, **52**, 3717–3720.
30 J. Zhou, L. Zhang and Y. Tian, *Anal. Chem.*, 2016, **88**, 2113–2118.
31 P. Huang, P. Rong, J. Lin, W. Li, X. Yan, M. G. Zhang, L. Nie, G. Niu, J. Lu, W. Wang and X. Chen, *J. Am. Chem. Soc.*, 2014, **136**, 8307–8313.
32 J. Lin, M. G. Zhang, Y. Tang, B. Wen, H. Hu, J. Song, Y. Liu, P. Huang and X. Chen, *Nanoscale*, 2016, **8**, 7430–7434.

